ISES International Solar Energy Society

Conference Proceedings

EuroSun 2014
Aix-les-Bains (France), 16 – 19 September 2014

Modeling of direct steam generation linear concentrating solar plants: dynamic studies

Antoine Aurousseau[1,2], Valéry Vuillerme[1] and Jean-Jacques Bezian[2]

[1] Univ. Grenoble Alpes, INES, F-33375 Le Bourget du Lac, France

CEA, LITEN, Laboratoire des Systèmes Solaires Haute Température, antoine.aurousseau@cea.fr;

[2] Université de Toulouse, Mines Albi, CNRS, Centre RAPSODEE, France.

Summary

Concentrating solar power (CSP) using direct steam generation is a promising technology for renewable electricity generation. Power plants or solar fields applying this technology using linear concentrators and absorbers are already in operation in Spain, Australia, and Thailand. The natural transient condition of solar irradiation and two-phase flow in the absorber tubes result in a strongly dynamic behavior of the steam generation system. This dynamic behavior has to be studied for proper designing of the power plants. In this paper, a linear solar steam generator is modeled using the Modelica language and simulated using the Dymola software. The ThermoSysPro Modelica components library, developed by EDF (French electricity provider) is used and extended through further component developments. The dynamic behavior of the modeled linear solar steam generator is analyzed and compared to other models found in literature, and control strategies to ensure good operating conditions are addressed.

1. Introduction

According to the International Energy Agency, with appropriate support, concentrating solar power contribution to the global electricity production could reach 11.3% by 2050 (OECD/IEA, 2010). Although most commercial CSP plants use synthetic oil as heat transfer fluid, direct steam generation (DSG), which uses water/steam as heat transfer fluid, is a promising technology to be applied in CSP plants. It allows the heat transfer fluid to be fed directly into the steam turbine for electricity generation, without the need for heat exchange stages. Previous studies comparing oil and DSG have demonstrated that using DSG can lead to a reduction of the levelized electricity cost, up to 11% (Feldhoff et al., 2009, Eck et al., 2008). The presence of two-phase flow inside the absorber tubes provides good heat transfer coefficients, but is also a drawback because it increases the magnitude of the dynamic phenomena, which are already strong in CSP plants. To allow proper design and operation of DSG plants, those dynamic phenomena have to be studied, including through modeling and simulation. Steam turbines that are used in CSP plants are the same as those in nuclear or fossil fuel power plants, and require to be fed with steam at a temperature as constant as possible. This paper deals with the modeling and simulation of a linear solar steam generator and the study of its dynamic behavior and the necessary control strategies to allow for proper operating conditions. To model the solar steam generator, the Modelica language is used. Modelica is an object-oriented language that can model multi-physics systems. The ThermoSysPro library is used and further developed for the needs of the models. Previous work using the library has been carried out in the laboratory (Rodat et al., 2013). For interface and simulations, the commercial software from 3ds Dymola is used. The first part of this paper deals with the description of the solar steam generator that is modeled, with emphasis to its architecture, known as "recirculation" and which is found in the literature to be the most stable under transient irradiation. ThermoSysPro models are then described in a second part. The third part is dedicated to the dynamics analysis of the vaporizer section, with the aim of comparing results to the work of Eck & Hirsch (Eck & Hirsch, 2007). In the final fourth part, a simple control strategy for the solar steam generator is proposed and evaluated.

Selection and/or peer review under responsibility of EuroSun2014 Scientific Committee
doi:10.18086/eurosun.2014.12.01 Available at http://proceedings.ises.org

2. The modeled solar steam generator

Direct steam generation, as other technologies, is applied to both central receiver and linear receiver systems. Commercial DSG plants currently in operation use central tower technology, like Ivanpah SEGS in California, Fresnel linear receiver technology, like Puerto Errado 2 in Spain, and parabolic trough technology, like PSE-1 in Thailand. Between central receiver technologies and linear receiver technologies, thermo-hydraulic and control problematic are different, but they are close between linear Fresnel and parabolic-trough systems. This work deals with the modeling of a Fresnel receiver type solar steam generator, but it can applied to parabolic-trough receivers as well, since it does not deal with the optical parts. Only concentration ratios and overall collector efficiency are used for the design and modeling. Table 1 gives the details of the receivers for the vaporizer and superheater sections. Table 2 gives the operating conditions at nominal (design) point.

Table 1 : Vaporizer and superheater design parameters

	Vaporizer	Superheater
Length	257 m	234 m
Absorber tubes diameter	22.5 mm	42.91 mm
Absorber tubes thickness	2.87 mm	2.87 mm
Number of absorber tubes / row	7	3
Concentration ratio	50	50

Table 2 : Nominal operating conditions

DNI	1000 W/m²
Recirculation mass flow rate	1.41 kg/s
Vaporizet outlet steam fraction	0.7
Superheated steam mass flow rate	3.12 kg/s
Superheated steam temperature	450.8 °C
Solar field outlet superheated steam pressure	85 bar
Solar field outlet thermal power	10.15 MWth

2.1 Operation mode

Figure 1 shows a simple diagram of the modeled linear solar steam generator. It is operated in recirculation mode, which means that water is pre-heated and vaporized into saturated steam in a first solar field section, then superheated in another one. A phase separator between the sections separates the two phases, and liquid water is recirculated at the inlet of the vaporizer.

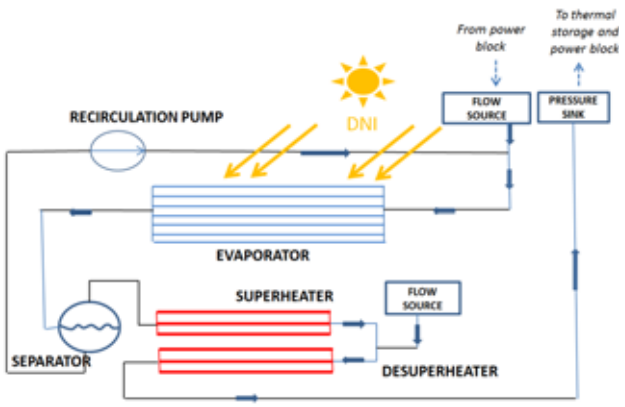

Figure 1: Simplified diagram of the modeled linear solar steam generator

Other operation modes, where water is vaporized and superheated in the same solar field section, exist. The "once-through" mode consists in feeding water at the inlet of the solar field, and the "injection" mode consists in injection of small flow rates all along the collector row, so that water is vaporized very fastly. To our knowledge, only a few studies have been carried out about that last operation mode. The once-through mode has been investigated, and it is the architecture chosen by Ausra (later Areva Solar) for their linear Fresnel solar fields. However, the most studied operation mode is recirculation. Studies have shown that it is more suited for handling irradiation transients with more simple control strategies (Valenzuela et al., 2004, Valenzuela et al., 2005).

2.2 Boundary conditions

At the vaporizer inlet, the feed water flow from the power block is mixed with the recirculation flow from the separator, and is modeled as a flow source. At the solar field outlet, the superheated steam flow fed to thermal storage and/or power block is modeled as a constant pressure sink. Thermal power on the absorber tubes is directly computed from the DNI, concentration ratios, and a collector global efficiency factor. The DNI nominal value used as design point is 1000 W/m².

3. Models

The object-oriented open-source Modelica language is used to model the solar steam generator. Acausal modeling allows for a direct writing of the systems equations. The open-source ThermoSysPro library, originally developed by the French electricity provider EDF for modeling conventional power plants, is used and further developed. Addressed below are the modeling of the two-phase flow in the tubes, the receivers, the pressures losses and the "desuperheater" injection. Details on other components models can be found in the ThermoSysPro 3.0 release (ThermoSysPro).

3.1 Absorber tubes two-phase flow modelling

Tubes are discretized only in the longitudinal direction, since ratio between length and diameter is very large. Pressure P and specific enthalpy h are state variables. Mass, energy, and momentum conservation equations, for each i cell of section A, diameter D and length dx, yields:

$$A\,dx\left(\frac{\partial \rho}{\partial h_{[i]}}\frac{\partial h}{\partial t}_{[i+1]} + \frac{\partial \rho}{\partial P_{[i]}}\frac{\partial P}{\partial t}_{[i+1]}\right) = Q_{[i]} - Q_{[i+1]} \tag{1}$$

$$A\,dx\left[\left(h_{i+1}\frac{\partial \rho}{\partial P_{[i]}} - 1\right)\frac{\partial P}{\partial t}_{[i+1]} + \left(h_{i+1}\frac{\partial \rho}{\partial h_{[i]}} + \rho_{[i]}\right)\frac{\partial h}{\partial t}_{[i+1]}\right] = h_{b\,[i]}Q_{[i]} - h_{b\,[i+1]}Q_{[i+1]} + dW_{[i]} \tag{2}$$

$$\frac{1}{A}\frac{\partial Q}{\partial t}_{[i]}\,dx = P_{[i]} - P_{[i+1]} - dpf_{[i]} - dpg_{[i]} - dpa_{[i]} \tag{3}$$

With the density ρ, pressure P, mass flow rate Q, cell boundary specific enthalpy h_b, exchanged thermal power dW, friction pressure loss dpf, gravity pressure loss dpg, acceleration pressure loss dpa. This last term is computed with homogeneous flow assumptions, and so is the gravity pressure loss term. On the other hand, friction pressure loss is computed using separate flows model, and computed as the product of the liquid only-pressure loss and a two-phase flow coefficient:

$$dpf_{2\varphi} = \emptyset_{LO}\; dpf_{LO} \tag{4}$$

Where dpf_{LO} is computed as the pressure drop with only liquid flowing at full rate. The coefficient $\emptyset_{LO}$ is computed with empirical correlation (ThermoSysPro).

The heat transfer coefficient in single-phase flow region is computed using Dittus-Boelter equation:

$$h_{[i]} = 0.023\frac{k_{[i]}}{D}Re_{[i]}^{0.8}\,Pr_{[i]}^{0.4} \tag{5}$$

In two-phase flow region, the heat transfer coefficient is computed using the superposition method:

$$h_{2\varphi\,[i]} = E_{[i]}\,h_{cl\,[i]} + S_{[i]}\,h_{eb\,[i]} \tag{6}$$

With the convective boiling term h_{cl} computed with (5), E its corrective term computed with a correlation to the Martinelli parameter and the boiling number. The nucleate term boiling term h_{eb} is computed with a specific correlation (ThermoSysPro), and its corrective term S computed as a function of E and the liquid Reynolds number. Flow properties are computed using the IF97 water/steam tables.

3.2 Receiver modelling

Figure 2 shows a simplified diagram of the modeled linear Fresnel receiver.

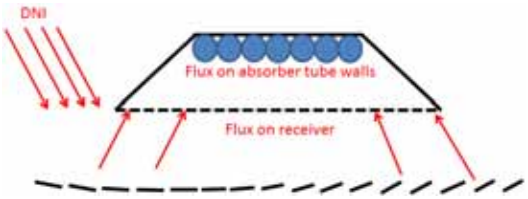

Figure 2: Simple diagram of the modeled receiver

Heat flux on the tube walls is computed with the following equation:

$$\phi = DNI\ FC\ \eta_g \pi\ D_e\ L\ n \quad (7)$$

With the direct normal irradiance DNI (W/m²), concentration ratio FC, the overall reflectors-receiver optical efficiency η_g, outer tubes diameter D_e, tube length L, and number of tubes n. The product of the last four terms is the computation of the total tubes external walls area. The modelled heat flux is homogeneous on the whole area, when only the bottom part of the tube surface actually receives the heat flux. Since this work focuses on the dynamic behavior with fast transients, another assumption is that the overall optical efficiency remains constant for the simulations time.

3.3 Pressure drops modelling

Pressures losses outside the absorber tubes are modelled with linear pressure drop components for the piping, and singular pressure drop components for the bends and junctions.

3.4 Desuperheater modelling

To ensure better superheated steam temperature stability, cold water is injected in the middle of the superheating part of the solar field. That injection is modelled as a fluid mixer with a simple enthalpy balance. The physics of the atomization is therefore not modelled here.

3.5 Influence of the tubes discretization

As previously discussed, tubes are discretized in the longitudinal direction. As the ThermoSysPro user can set the number of cells, its influence has been studied in preliminary simulations. Table 3 sums up the converged values of the output flows, computed for several numbers of cells. The water mass flow rate relative difference between the computations with 6 cells and 10 cells goes down to 0.41%, which is low. The meshing with 10 cells is therefore considered as fine enough for the simulations to come, and the computation cost is still low.

Table 3: Discretization influence study data

Converged computed mass flow rates	Steam (kg/s)	Water (kg/s)
3 cells	0.3229	2.1327
6 cells	0.3226	2.1511
Relative difference	*- 0.09 %*	*+ 0.86 %*
10 cells	0.3225	2.16
Relative difference	*- 0.03 %*	*+ 0.41%*

3.6 Influence of the dynamic tubes model options

Others simulations have been carried out to study the influence of the vaporizer tube options, available in the the ThermoSysPro model. Figure 2 shows the computed mass flow rates at the evaporator outlet, when it is

submitted to an irradiation step of -70% during at 96 seconds period (see next part). The influence of two particular options is evaluated: the acceleration pressure loss term dpa in the momentum balance equation and the dynamic density term $\frac{\partial \rho}{\partial t}$ in the energy balance equation. These two terms leads to more computation instabilities with the Dymola solvers, and it seems interesting to find out if they bring precision to dynamic simulations. Figure 3 shows that the three set of options leads to the same converged flow rates, but the liquid and steam peaks generated by the DNI step can only be seen with all options. The computed steam mass flow rate with the acceleration pressure loss term shows a peak of 4 kg/s after the DNI step, when nominal value is around 3.2 kg/s. Without this term in the equation, no such peak is computed. Although it might be difficult to be handled by the control system, we are interested in computing such a peak, since the purpose of this work is to study the dynamic behavior of the system. It seems therefore more appropriate to carry out simulations with full dynamic options in the models.

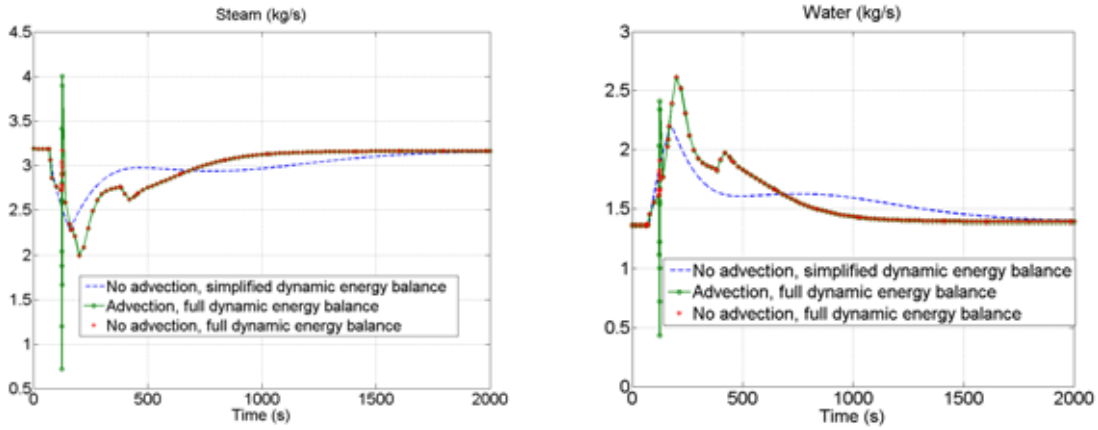

Figure 3: Influence of the evaporator tube model options on the computed outlet flow rate, when undergoing a DNI step

4. Vaporizer dynamics without control systems

For this part of study, only the vaporizer section is modelled, as it is the main driver of the dynamics related to water and steam mass flow rate in the solar field (Eck & Hirsch, 2007). For the sake of simulations stability, preliminary simulations are carried out for the whole solar field to slowly reach nominal operating conditions. Once stability is achieved and nominal conditions are reached, computation variable are used as starting points for the actual simulations. In these simulations, a simple pressure sink models the downstream part of the solar field (separator, superheater, etc.). Its value is obtained from the vaporizer outlet pressure computed at nominal conditions for the full solar field simulation. The recirculation flow at the vaporizer inlet is modelled as a flow source.

Comparison is made with the results of Eck & Hirsch (Eck & Hirsch, 2007), in which the vaporizer of a parabolic-trough solar field is modelled. Table 4 sums up the operating conditions for the simulations.

Table 4 : Studies operating conditions and vaporizer parameters

	Eck & Hirsch	Study
Nominal DNI	850 W/m²	1000 W/m²
Evaporator length	800 m	257 m
Number of tubes/row	1	7
Tube inner diameter	0.055 m	0.0225 m
Tube wall thickness	7.5 mm	2.87 mm
Recirculation mass flow	0.25 or 1.0 kg/s	1.412 or 2.824 kg/s
Feedwater mass flow and temperature	1.2 kg/s – 125°c	3.12 kg/s – 100°c
Operating pressure	70 bar	112 bar

4.1 Step in the feed water mass flow rate

A change in the feed water mass flow rate is simulated with the Dymola-ThermoSysPro vaporizer model, to

get a general impression of the system behavior. Comparison is made with Eck & Hirsch. To compute the Eck & Hirsch study density at the vaporizer outlet, simulations data are used. Steam fractions are estimated from the plots (shown on figure 4) of the water mass flow rate evolution at the outlet:

$$x = 1 - \frac{Q_w}{Q_{total}} \tag{8}$$

with Q_w the liquid water mass flow rate at stationary conditions, and Q_{total} the sum of the recirculation mass flow rate and the feed water mass flow rate at the inlet.

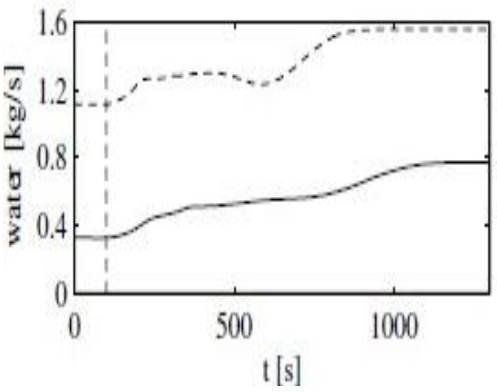

Figure 4 : Water mass flow at evaporator outlet for recirculation mass flow of 0.25 kg/s and 1 kg/s, extracted from Eck & Hirsch (Eck & Hirsch, 2007)

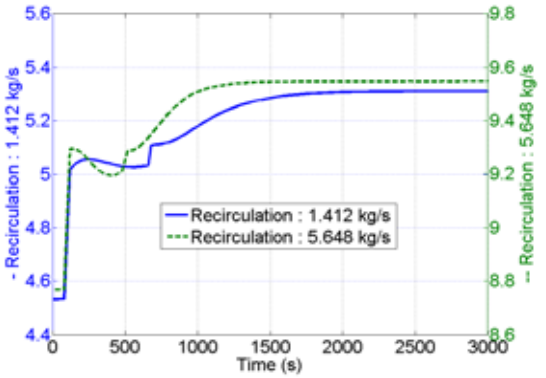

Figure 5 : Two-phase flow rate (kg/s) at evaporator outlet for the Dymola-ThermoSysPro study

For the computation of the mean velocities and residence time of the Eck & Hirsch study, it is assumed that the recirculation flow is at liquid saturation conditions, which depends on the operating pressure, assumed to be constant through the whole loop. We also use the assumption made by Eck & Hirsch that the two-phase flow is homogeneous. Based on this last assumption, the average density at vaporizer outlet is computed with the following equation (Eck & Hirsch, 2007):

$$\rho = 1/\left[\frac{1}{\rho'} + x\left(\frac{1}{\rho''} - \frac{1}{\rho'}\right)\right] \tag{9}$$

with $\rho'$and ρ'' the densities at saturation conditions, respectively for water and steam. The overall flow density in the vaporizer tube is then computed as the average of the density at inlet conditions (mixing of saturated water and feed water) and outlet conditions. Mean velocities in the vaporizer are then computed:

$$V_{mean} = \frac{4Q}{\rho_{mean}\pi D} \tag{10}$$

with Q the mass flow rate in the tube and D the tube diameter. Residence times are then computed:

$$\tau = \frac{L}{V_{mean}} \tag{11}$$

Table 5 : Feed water step reaction analysis

	Eck & Hirsch		Dymola-ThermoSysPro	
Step in the feed water mass flow rate	1.2 to 1.5 kg/s (+25%)		3.12 to 3.9 kg/s (+25%)	
Recirculation mass flow rate	0.25 kg/s	1.0 kg/s	1.412 kg/s	5.648 kg/s
Estimated mean velocity	1.5 m/s	2.17 m/s	0.96 m/s	1.76 m/s
Estimated residence time	534 s	368 s	268 s	146 s
Time to new stationary conditions	1075 s	775 s	2660 s	1780 s
Change in the time to reach stationary conditions	100%	-28%	100%	-33%

Figure 5 shows the plots of the Dymola-ThermoSysPro study. Table 5 collects the results of both studies.

The change in the feed water mass flow rate leads to a change in the flow balance and energy balance of the evaporator. In the Eck & Hirsch study, it takes about twice the residence time in the evaporator to reach stationary conditions after the step, and increasing the recirculation mass flow rate by a factor 4 reduce this settling time by 28%. For the Dymola – ThermoSysPro study, it takes about 10 times the residence time to reach stationary conditions again after the step. This indicates that the evaporator architecture that is simulated has bigger time constants than the one simulated by Eck & Hirsch, and the dynamic phenomena induced by two-phase flows and dynamic energy transfers have a stronger influence with this architecture. To compare thermal inertias of both vaporizer architectures, the tubes mass of steel is calculated, using data in table 4, and assuming that the tube walls are made of stainless with a density of 8000 kg/m^3. The mass of steel in the tubes in the modelled vaporizer is about 13.2 tons, and about 9.4 tons for the vaporizer row in the Eck & Hirsch study. This difference can also explain the larger time constants, especially the settling time, in the modelled Fresnel architecture. However, a common finding is that increasing the recirculation flow rate by factor 4 decreases the settling time by about 30%.

4.2 Irradiation disturbance tests

Simulations are carried out to study the dynamic reactions of the evaporator to irradiation fast transients. The triple irradiation disturbance test of Eck & Hirsch is applied to the modelled evaporator. Figure 6 shows the signal that is used in Eck & Hirsch work, which is used with the Dymola-ThermoSysPro simulations. Table 6 gives the simulations parameters.

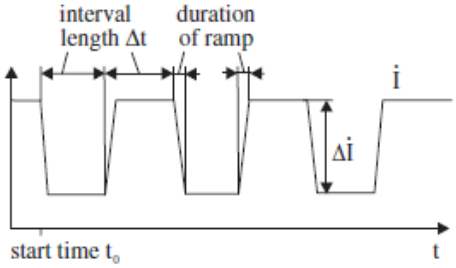

Figure 6 : Eck & Hirsch triple disturbance test signal

Table 6: Triple irradiation disturbance test data

	Eck & Hirsch			Dymola – ThermoSysPro		
Feed water flow rate (kg/s)	1.2	1.2	1.2	3.12	3.12	3.12
Recirculation flow rate (kg/s)	0.25	0.25	0.25	1.412	1.412	1.412
Δt (s)	30	120	240	12	48	96
% of residence time	4.6 %	18.4 %	36.8 %	4.6 %	18.4 %	36.8 %
Ramp duration (s)	5 s	5 s	5 s	5 s	5 s	5 s
ΔI (W/m²)	-875	-600	-600	-1000	-700	-700
% of normal irradiation	-100 %	-70 %	-70 %	-100 %	-70 %	-70 %

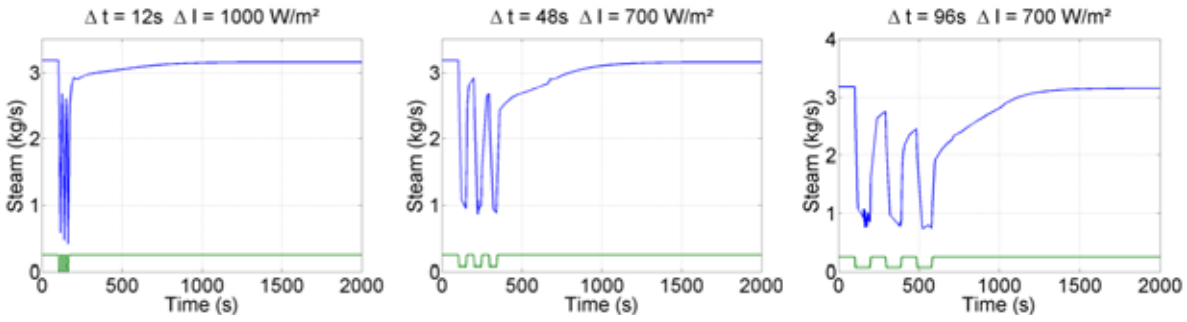

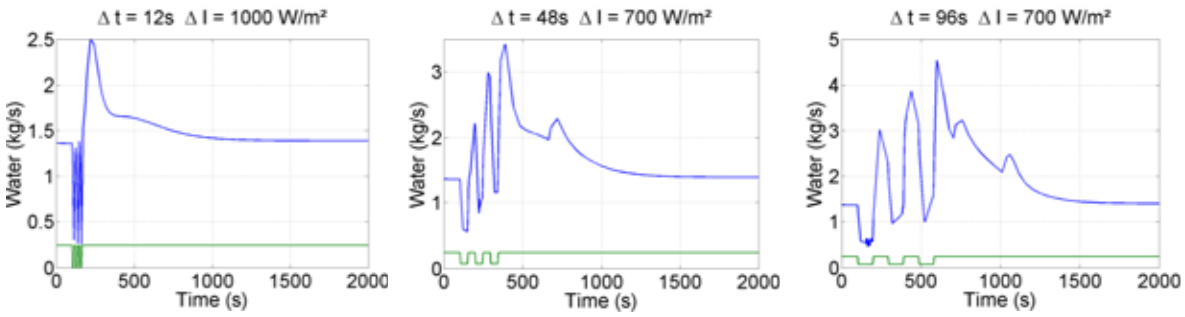

Figure 7: Reaction of the modelled evaporator to triple irradiation disturbance

In order to make good comparison with Eck & Hirsch data, the time characteristics of the disturbance are chosen to be equally proportional to the estimated residence time of the two-phase flow in the tubes (see table 5), and ramp durations are chosen to be the same. DNI transient are also equally proportional to their respective nominal values. Figure 7 shows steam and water mass flow rate reactions to the three irradiation transients. As it has been seen with figure 3 and the model options study, it takes more than 1500 s to reach stationary conditions again after a disturbance. Therefore, the effects of the 3 consecutive DNI disturbances we are studying here overlap. General good agreement for the mass flow rates behavior is found with Eck & Hirsch results (Eck & Hirsch, 2007). Largest water flow peaks are found to be around 4.5 kg/s, which is about 3 times the nominal value. This is less than Eck & Hirsch (8 times the nominal value). The situation where two liquid peaks happen after the DNI disturbance (the first one being due to the sudden drop of vapor fraction at the outlet, and the second one to the sudden increase in irradiation and its steam-induced liquid blow out) is also visible with our computations, but the second peaks are not as large as in Eck & Hirsch study. This is once again partly due to the larger thermal inertia of the Fresnel receiver. General conclusion is that good agreement is found between the two models, and the vaporizer that is modelled with Dymola-ThermoSysPro seems to have a larger thermal inertia and a smoother dynamic behavior.

5. Dynamics of the solar field with control system

For this part of the study, simulations of the whole solar field are carried out. We compare its dynamic response to fast irradiation transients with and without control systems, and some details are addressed about how the control system is designed.

5.1 Control strategies

As previously mentioned, DNI disturbance simulations start from operating nominal conditions, which were also used as design point for the sizing of the modeled solar field. The term “nominal” is purely fictional: as solar irradiation is constantly changing, both in a slow and deterministic way (daily and yearly cycles) and in a fast and unpredictable way (clouds disturbance), input energy on the solar steam generator is never constant. This is a challenge for the design of both the solar field and its control system. Figure 8 shows the control loops that are proposed in this study.

Recirculation mass flow rate is maintained constant by controlling the recirculation pump rotational speed: pressure and steam quality fluctuations upstream of the pump generate fluctuations in the flow at the inlet. The rotational speed therefore has to be adjusted to maintain a constant flow rate.

Steam fraction at the vaporizer outlet is controlled by adjusting the feed water flow rate, as the mixing between recirculation saturated water and “fresh” feed water determines the outlet steam fraction, for a given heat flux on the tube walls. The model uses a steam quality sensor, which is developed for the need of this study and uses a simple computation of the steam fraction from the state variables (pressure and enthalpy) and steam tables. There are to our knowledge no such sensors in reality, as real-time field measurement of steam quality is only available through very elaborated technologies. However, the value can be computed through an energy balance. Using this sensor in the models is convenient for a direct control on the steam fraction (thus avoiding dry-out in the vaporizer tubes) and on the recirculation pump power consumption.

Finally, the superheated steam control loop adjusts the flow injection in the superheater to control the outlet temperature. All loops use simple feedback with a PI controller.

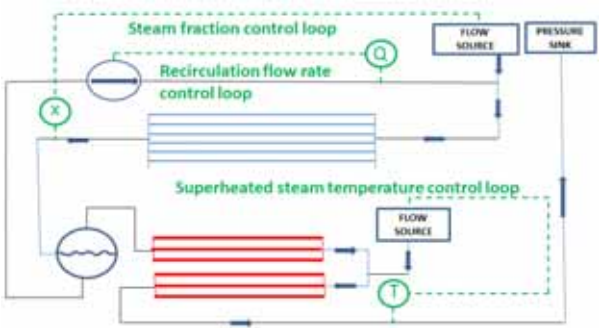

Figure 8: Diagram of the proposed control loops

Controller parameters are computed with an open loop step reaction method. For each loop, the control parameter is given a step disturbance and a process model is then fit to the reaction plot of the controlled variable. PI controller parameters are then computed according to the fitted model parameters. This method gives good order of magnitude for the PI parameters, and they are then manually adjusted to get the best performance. To illustrate the methodology, figure 9 shows the open-loop reaction of the superheater outlet steam temperature to a 20% step increase of the desuperheater injection flow rate. The fitted first order model that is used to compute the PI controller parameters is also plotted. Figure 10 is the plot of the temperature reaction to a +30°C step change in the setpoint, to evaluate the obtained controller performance.

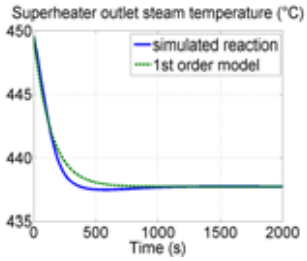

Figure 9 : Superheated steam temperature reaction to a 20% step change in the injection flow rate

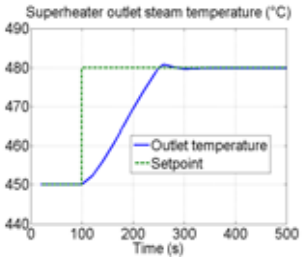

Figure 10 : Superheated steam outlet temperature reaction to a setpoint step change, with PI control (k=0.22, Ti=80s)

Table 7 sums up the parameters for the designed control loops.

Table 7 : Control loops parameters

Control loop	Fitted model	PI parameters	Setpoint
Recirculation mass flow rate	Simple gain k =588	K = 588, Ti = 60	4.12 kg/s
Vaporizer outlet steam fraction	1st order, $\frac{-0.72}{1+840p}$	K= -936, Ti = 840	0.7
Superheater outlet steam temperature	1st order, $\frac{-295}{1+140p}$	K = -0.38, Ti = 140	450 °C

5.2 Simulations results

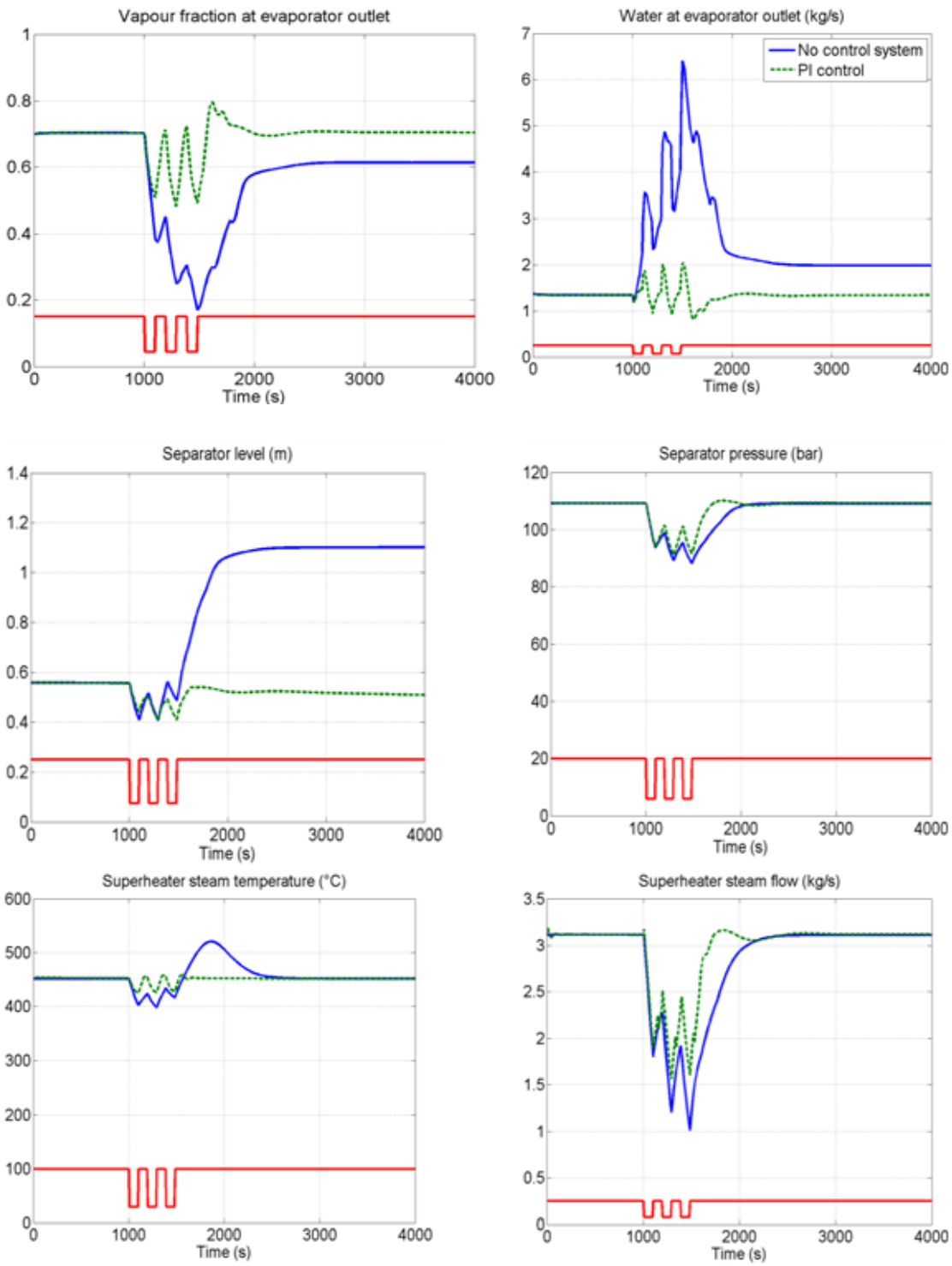

Figure 11: solar field response to fast irradiation transients with PI control (-) and without (--). $\Delta t = 96s,\ \Delta I = -700\ W.m^2$

Figure 11 shows the solar field variables response to the triple irradiation disturbance. (see previous part). Plotted are the vaporizer outlet steam fraction and liquid water flow rate (directly computed from the steam fraction), the separator pressure and liquid water level, and the superheater outlet steam flow rate and temperature. Nominal stable operating conditions from which the simulations start are those given in table 2.

It can be seen that without control system, steam fraction and separator level reach new stable conditions after the disturbances when DNI is back to normal. That is not satisfactory since the solar field no longer works at design point with the same solar irradiation. The vaporizer control loops stabilize both outlet steam fraction and separator water level after disturbances. It also strongly diminishes the magnitude of the fluctuations in the steam quality in the vaporizer tubes, which leads to smaller liquid flow peaks in the separator. The magnitude of the separator pressure and the steam flow rate fed to the superheating section are

also decreased with the control loops, but only slightly if compared to the transients without control systems. They are indeed mainly driven by solar irradiation, and the control system can only have a small influence on these quantities.

The superheated steam temperature control loop also has a positive influence on the temperature fluctuations. The plot on figure 11 shows that the peak above 550°C, that happens with no control system after solar irradiation gets back to normal, does not happen with the controlled desuperheater. Outlet temperature does not exceed 457°C. However, the control system for this loop is not efficient enough, because the transients' magnitudes are too high for the steam to be directly fed to a power block turbine. It can be seen that the temperature drops 27°C in less than 100 seconds. That gradient is too large, and the net change in the temperature is too high as well. More elaborated control has to be designed.

6. Conclusion and perspectives

A simple linear solar steam generator using Fresnel receiver architecture and a recirculation operation mode was developed and simulated. ThermosSysPro models for water/steam fluid components were used and evaluated for this purpose. Dynamic behavior of the vaporizer section was simulated and the results were compared to a reference study (Eck & Hirsch, 2007) for evaluating the model. Good general behavior agreement is found between the two models, although a larger thermal inertia of the modelled Fresnel architecture seems to be shown in the results. Dynamic behavior of the whole solar field was simulated under fast irradiation transients. Results show that control loops for the vaporizer are satisfactory for this particular design and operating conditions, but also that the superheater steam temperature control loop is not efficient enough to handle fast irradiation transient. Further studies have to be carried out to evaluate and propose more complex control systems. Strategies proposed in previous reference studies (Valenzuela et al., 2004, Valenzuela et al., 2005, Eck & Hirsch, 2007) will be evaluated for a use with our models, and strategies including the use of short-term irradiation prediction will be investigated, which is the perspective of this work.

7. References

Eck, M., & Hirsch, T. (2007). Dynamics and control of parabolic trough collector loops with direct steam generation. Solar Energy, 81, 268-279.

Eck, M., Benz, N., Feldhoff, F., Gilon, Y., Hacker, Z., Müller, T., Riffelmann, K-J., et al. (2008). The potential of direct steam generation in parabolic troughs - results of the German project DIVA. Proceedings of the 14th Biennal CSP SolarPACES Symposium.

Feldhoff, J. F., Eck, M., Benitez, D., & Riffelmann, K-J. (2009). Economic Potential of Solar Thermal Power Plants with Direct Steam Generation compared to HTF Plants. *Proceedings of the ES2009 Conference* (pp. 663-671).

OECD/IEA. (2010). Technology Roadmap, Concentrating Solar Power.

Rodat, S., Souza, J. V. D., Thebault, S., Vuillerme, V., & Dupassieux, N. (2013). Dynamic simulations of Fresnel solar power plants. *Proceedings of SolarPACES2013*.

ThermoSysPro 3.0 Open Source Release.

Valenzuela, L., Zarza, E., Berenguel, M., & Camacho, E. F. (2004). Direct steam generation in solar boilers, using feedback to maintain conditions under uncontrollable solar radiations. IEEE Control Systems Magazine, 15-29.

Valenzuela, L., Zarza, E., Berenguel, M., & Camacho, E. F. (2005). Control concepts for direct steam generation in parabolic troughs. Solar Energy, 78, 301-311.